Int. J. Electrochem. Sci., 6 **(2011)** 6670 - 6681

International Journal of
ELECTROCHEMICAL
SCIENCE
www.electrochemsci.org

Synthesis and Electrochemical Feature of a Multiple-Phases Li-Rich Nickel Manganese Oxides Cathode Material

Jun Wang, Yonggao Xia[*]*, Xiayin Yao, Minghao Zhang, Yiming Zhang, Zhaoping Liu*[*]

Ningbo Institute of Material Technology & Engineering, Chinese Academy of Sciences, Ningbo, 315201, P. R. China.
[*]E-mail: xiayg@nimte.ac.cn, liuzp@nimte.ac.cn

Received: 7 October 2011 / *Accepted:* 15 November 2011 / *Published:* 1 December 2011

A cathode material with multiple phases, containing Li_2O-deficient layered Li-rich nickel manganese oxides and spinel $LiNi_{0.5}Mn_{1.5}O_4$, was prepared by controlling the calcination temperature. It is believed that the lixiviation of Li_2O resulted in the phase separation of the final product when the calcination temperature was higher than 900 °C. Compared with pure-phase $Li_{1.2}Ni_{0.2}Mn_{0.6}O_2$ sample, the multiple-phases sample had a lower initial irreversible capacity (around 25 mAh g^{-1}). Only for the multiple-phases sample, it exhibited an increasing capacity with cycles in the voltage range of 2-4.8 V both at 25 °C and 55 °C. It is treated that the activation of the lithium ion conduction pathway during cycling, accompanied with the growing amount of redox reaction sites of Ni^{4+}/Ni^{2+} and Mn^{4+}/Mn^{3+} and reducing charge transfer resistance, contributed to the increasing capacity of the cell with cycle number.

Keywords: lithium ion battery, cathode material, layered Li-rich, lithium nickel manganese oxide

1. INTRODUCTION

Lithium ion batteries (LIBs) have aided the portable electronics revolution during the past two decades because they store much higher energy per unit weight or volume compared with other rechargeable battery systems. Most of the LIBs are still using $LiCoO_2$ as the positive electrode, and graphite as the negative electrode; however, the high cost of cobalt and the relatively low practical capacity of $LiCoO_2$ (~ 140 mAh/g) inhibits its further use in price-sensitive applications [1, 2]. In comparison, despite the abundance of iron and manganese, the capacities of spinel $LiMn_2O_4$ and olivine $LiFePO_4$ are limited in satisfying the demands of high energy density [3, 4]. These difficulties have generated considerable worldwide efforts to seek new cathode materials with higher energy density. In this regard, lithium- and manganese- enriched oxides, which are the solid solutions between

layered $Li[Li_{1/3}Mn_{2/3}]O_2$ (also designated as Li_2MnO_3) and $LiMO_2$ (M=Mn, Ni, and Co), recently have received much attention as they exhibit specific capacities as high as 250 mAh/g [5-8]. However, these integrated materials usually suffer large irreversible capacity (IRC) loss at the first cycle and poor capacity retention, which are the main obstacles against the application of these materials [9].

Recently, Belharouak *et al.* [10] proved the presence of the high voltage spinel $LiNi_{0.5}Mn_{1.5}O_4$ phase within some layered Li-rich solid solutions. The discharge capacities of these impure solid solutions increased with cycles between 2.0 and 5.0 V in the initial several cycles, and the IRC loss was around 10 ~ 75 mAh g^{-1}, which was much lower than the common value of 120 mAh g^{-1} [11]. Similar phenomena of increasing capacity in the phase-separation sample were also reported [12, 13]. However, so far as we know, the temperature-controlled parameters for synthesizing such multiple-phases sample with lower IRC values are absent. Moreover, the detailed study is necessitated in order to understand the mechanism of increasing capacity in the solid solution cathode materials with low irreversible capacity loss cycled between 2.0 and 4.8 V.

In this work, a multiple-phases cathode material of Li-rich nickel manganese oxides was investigated with respect to its synthesis parameters, the valence states of transition metal ions, and the room- and high-temperature charge/discharge behavior. According to the above results, associated with the cyclic voltammetry (CV) and electrochemical impedance spectroscopy (EIS) tests, the possible mechanism of the phenomenon of increasing capacity was discussed properly.

2. EXPERIMENTAL

In a typical synthesis of Li-rich nickel manganese oxides, 500 ml of mixed aqueous solution of $Ni(NO_3)_2$ and $Mn(NO_3)_2$ (the concentration of total metal ions was 0.1 M, and the molar ratio of Ni:Mn = 1:3) was pumped into a continuous stirred reactor, and then stoichiometric amount of LiOH aqueous solution was added in dropwise. The resultant slurry was stirred for one hour, and then was spray-dried with the inlet air temperature of 200 °C and the exit air temperature of 100 °C. The as-prepared precursor was firstly pre-heated at 450 °C for 5 h under air, and then calcined at higher temperature 1000 °C for another 5 h. The heating rate was maintained at 4 °C min^{-1}.

The thermo evolution of the mixed precursor was studied by a thermogravimetric/differential thermal analyzer (Pyris Diamond TG/DTA, Perkin-Elmer) with heating rate of 4 °C min^{-1}, within the temperature range of 25-1200 °C. X-ray powder diffraction (XRD) measurements were performed using an AXS D8 Advance diffractometer (reflection θ-θ geometry, Cu Kα radiation, receiving slit 0.2 mm, scintillation counter, 40 mA, 40 kV) from Bruker, Inc. (Germany). The chemical compositions of the products were confirmed quantitatively by inductive coupled plasma (ICP) with an emission spectrometer (Optima 2100 DV, Perkin-Elmer). The scanning electron microscopy (SEM) images were taken with an S-4800 field emission scanning electron microscope (15 kV, Hitachi, Japan). X-ray photoelectron spectroscopy (XPS) measurements were performed using an AXIS Ultra DLD spectrometer (Japan). All of the spectra were collected using a monochromatic Al-Kα radiation (1486.6 eV) X-ray source operated at 150 W, and at the pass energy of 10 eV. Curve fitting of slow-scanned XPS spectra was carried out using a peak-fit program with a Gaussian–Lorentzian sum

function. The C 1s peak (284.6 eV) from the adventitious carbon was used as the reference for binding energy calibration.

Electrochemical measurements were carried out on CR2032-type coin cells. The cathode electrodes were made of 80 wt.% active materials, 10 wt.% acetylene black, and 10 wt.% polyvinylidene fluoride (PVDF). The areal density of the active material was around 5 mg cm^{-2}. Lithium metal flake was used as the anode. A Celgard 2502 membrane was used as a separator. The electrolyte was composed of 1 M LiPF6 solution in ethylene carbonate (EC)/dimethyl carbonate (DMC) (1:1 by volume). The cells were assembled in an argon-filled glove box and were tested in the voltage range of 2 - 4.8 V with LAND-CT2001A battery test system (Jinnuo Wuhan Corp., China). The cyclic voltammetry (CV) was performed with an Autolab PGSTAT302N (Metrohm, Switzerland) controlled by a desktop PC. The electrochemical impedance spectroscopy (EIS) measurements were conducted by Autolab83710 impedance analyzer with an amplitude voltage of 10 mV and frequency range of 0.001 Hz-0.1 MHz.

3. RESULTS AND DISCUSSION

Thermal analysis data of the spray-dried precursor containing Li, Ni, and Mn etc. elements is shown in Fig. 1.

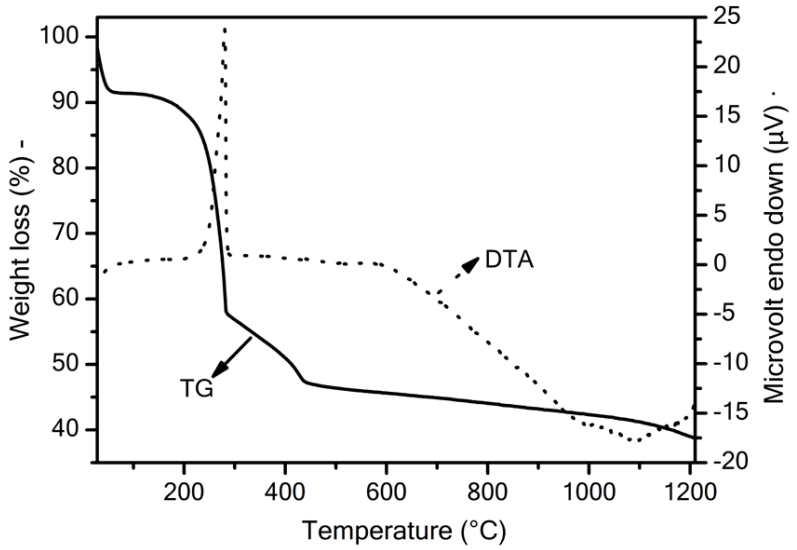

Figure 1. Thermo gravimetric analysis profile for the spray-dried precursor recorded at a heating rate of 4 °C min^{-1}

TG trace exhibits three distinct weight loss steps and the DTA curve shows an endothermic peak and two exothermic peaks. From the TG trace, there is about 8.2% weight loss when the sample is heated to 100 °C, which is mainly due to the removal of the adsorbed water. The accompanied

endothermic peak below 100 °C is weak, indicating that the most of the crystal water and adsorbed water have been removed by the spray-drying process. Between 100 and 450 °C, about 45.1% weight loss is associated with decomposition of nitrate and hydroxyl ions, accompanied by an exothermic peak around 281 °C. There are some weight loss above 450 °C, especially when the temperature is higher than 1000 °C, and a noticeable exothermic peak around 1000 °C. Hence, it is essential to further study the formation of the lithium nickel manganese oxides compound around 1000 °C, as well as the relevant electrochemical feature.

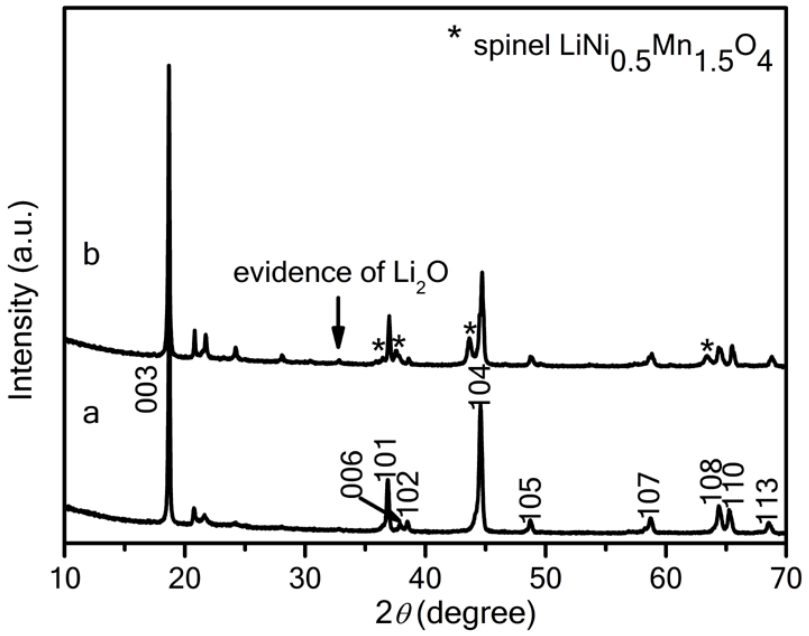

Figure 2. XRD patterns of Li-rich nickel manganese oxides samples prepared at (a) 900 °C, and (b) 1000 °C

Fig. 2 shows the XRD patterns of Li-rich nickel manganese oxides samples prepared by calcining at 900 °C and 1000 °C. It can be seen from Fig. 2a, all of the peaks can be indexed as a hexagonal α-$NaFeO_2$ structure (space group: *R-3m*, No. 166), except for a few broad peaks between 20 ° and 25 °. Na and Fe sites in α-$NaFeO_2$ type structure are occupied by lithium ions, and transition metal ions or a mixture of lithium and transition metal ions in these materials, respectively, *i.e.*, the composites are built up from alternative lithium layer and transition metal oxides (MO_2) layer or the layer containing the mixture of lithium and M ions. The appearance of the diffraction peaks between 20° and 30° is due to the super lattice ordering of Li and Mn in the transition metal layers for layered Li-rich solid solution materials [14, 15].

The miller indices of the peaks are demonstrated in the lower panel. The separations of the (006)/(102) and (108)/(110) peaks for hexagonal structure indicates the formation of ordered lamellar structures [16]. The separations of the (006)/(102) and (108)/(110) peaks are distinct, which indicates

the formation of highly ordered lamellar structures. From the ICP results, the formula of the sample prepared at 900 °C can be expressed as $Li_{1.2}Ni_{0.2}Mn_{0.6}O_2$.

Yoncheva *et al.* reported that heating the ex-carbonate $LiNi_{0.5}Mn_{0.5}O_2$ at 950 °C for 12 h led phase separation of final product [17]. In our experiments, as increasing the calcining temperature to 1000 °C, there was a phase separation, which was reflected by additional peaks in its XRD pattern (marked by asterisk in Fig. 2b). In order to verify the fact that the phase separation can occur in the samples at high temperature regardless of the synthesized route, we also have performed the experiments similar to the method of *ref.* 6 (co-precipitation) and *ref.* 10 (solid state reaction), except that the calcining procedures were as follows: pre-heated at 450 °C for 5 h under air and then calcined at 1000 °C for another 5 h. The XRD patterns of the as-prepared samples were similar with Fig. 2b, indicating that the phase separation also occurred (see Fig. S1). Belharouak *et al.* [10] identified that the impure phase was spinel $LiNi_{0.5}Mn_{1.5}O_4$. From the ICP results, we found that the content of lithium decreasing with the increase of the calcination temperature (when > 900 °C). The XRD pattern in Fig. 2b reveals the presence of Li_2O (marked by arrow). Hence, we assumed that the overhigh calcining temperature had caused the evaporation of lithium and the surface lixiviation of Li_2O. Hereby, the deficiency of lithium at the surface led the formation of spinel $LiNi_{0.5}Mn_{1.5}O_4$ at the shell of the sample.

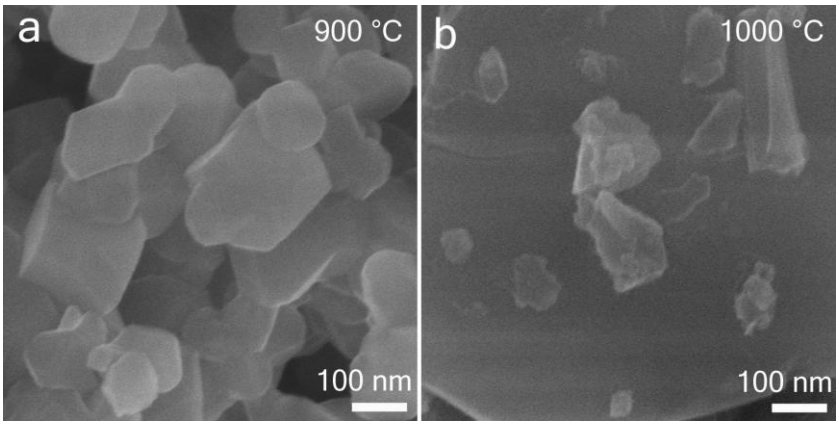

Figure 3. SEM images of the Li-rich nickel manganese oxides samples prepared at (a) 900 °C and (b) 1000 °C

Fig. 3a and 3b show SEM images of the Li-rich nickel manganese oxides samples prepared at 900 °C and 1000 °C, respectively. As observed, the sample prepared at 900 °C has a smooth surface with particle size in the range of 100-200 nm, whereas the sample prepared at 1000 °C is composed of micro-sized particles with a rough surface. According to the results of XRD and ICP, we strongly suggested that the rough surface of the microparticles was caused by the surface lixiviation of Li_2O and phase separation into $LiNi_{0.5}Mn_{1.5}O_4$ and Li_2O deficient Li-rich nickel manganese oxides under the high calcination temperature (1000 °C).

To confirm the valence states of the transition metals, XPS measurements were carried out on the samples with single/multiple phases. The Shirley-type background was subtracted from the

measured data, and curve fitting was performed with a combination of Gaussian (30%) and Lorentzian (70%) distribution.

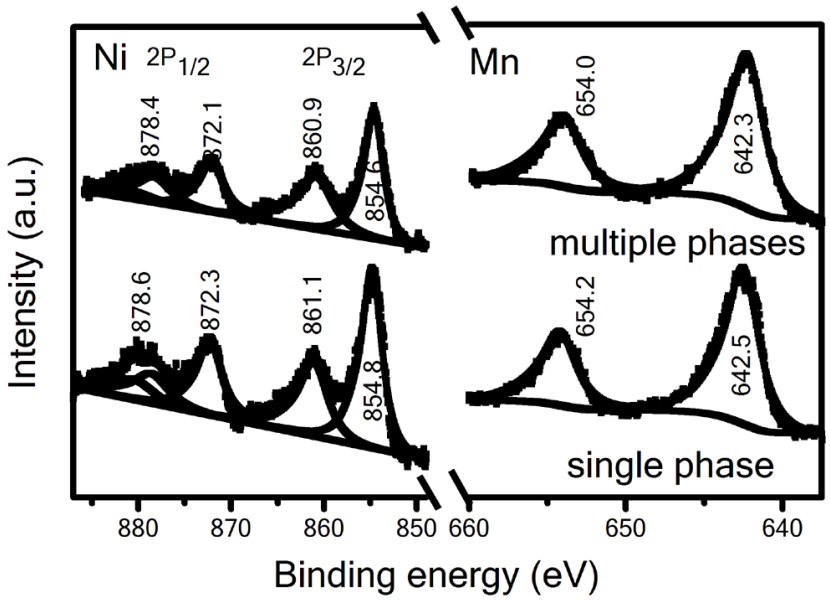

Figure 4. XPS 2p core-level spectra of Ni and Mn for the Li-rich nickel manganese oxides with single phase and multiple phases

Fig. 4 shows the XPS 2p core-level spectra of Ni and Mn ions in as-prepared samples. For both samples, the Mn $2p_{3/2}$-Mn $2p_{1/2}$ doublets are visually symmetric and can be well fitted with a single peak. The binding energies of Mn $2p_{3/2}$ are 642.5 eV and 642.3 eV, respectively. The values are very close to that (642.4 eV) of Mn $2p_{3/2}$ in λ-MnO_2 [18]. Therefore, it is believed that the Mn ions in the samples were predominantly in 4+ valence state. Although there was a phase separation for the sample prepared at 1000 °C, the valence state of Mn ions kept unalternated. The Ni 2p spectra are characterized by broad Ni $2p_{3/2}$-Ni $2p_{1/2}$ doublets. Similarly, each of these peaks fits with a single peak, which corresponds to Ni^{2+}. The peaks around 861.0 eV and 878.5 eV are considered to be the satellite peaks. For transition metal cations, the appearance of such satellite peaks has been explained to be the multiple splitting in the energy bands which results in a main peak of fundamental state and a satellite peak of higher energy corresponding to the excited state [19].

The electrochemical charge/discharge measurements of the samples were carried out using Li metal as an anode in the voltage range of 2.0-4.8 V. Fig. 5 shows the comparative cycling performances of as-prepared Li-rich nickel manganese oxides under a current density of 12.5 mA g^{-1}. For the single-phase $Li_{1.2}Ni_{0.2}Mn_{0.6}O_2$, it delivers an initial discharge capacity of 260 mAh g^{-1}, and the capacity retention is about 80 % after 50 cycles. The multiple-phases sample exhibits a distinct phenomenon of the increasing capacity with the cycle number in the initial cycles. Its discharge capacity increases dramatically from the initial value of 76 mAh g^{-1} to 210 mAh g^{-1} at 10^{th} cycle, and further increases gradually to a stable capacity of over 250 mAh g^{-1} after 24^{th} cycle. As reported in *refs.* 10 and 13, the samples prepared at 900 °C for 20 h, of which the phase-separation level should be

lower than the sample prepared at 1000 °C, also had a phenomenon of increasing capacity, although their samples had a relatively larger initial capacity associated with the less degree of phase separation. Thereby, we believed that the phase separation was responsible for the phenomenon of increasing capacity. The multiple-phases sample had a high discharge capacity of 250 mAh g^{-1} after 50 cycles, while for the single-phase sample, it only delivered a capacity of lower than 200 mAh g^{-1}.

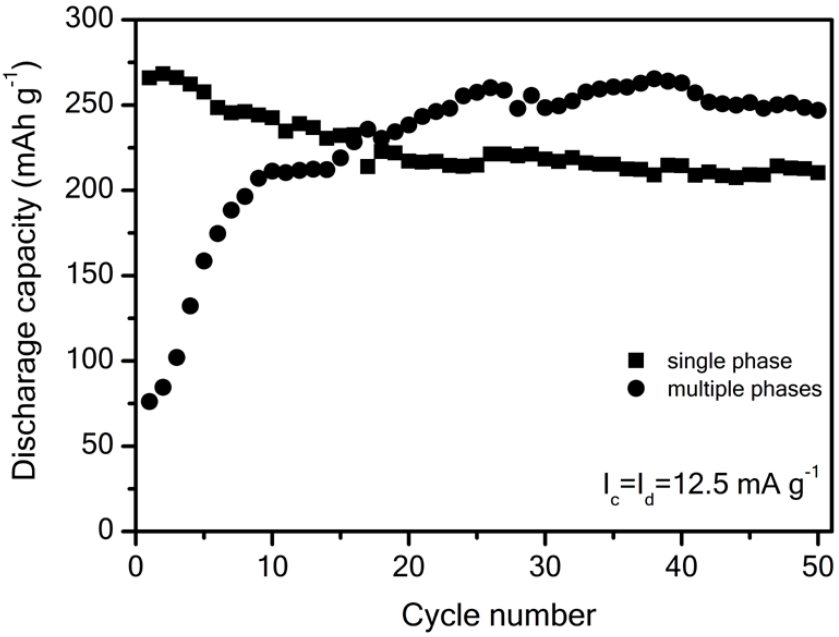

Figure 5. Comparative cycling performances of the Li-rich nickel manganese oxides with single phase and multiple phases, under 12.5 mA g^{-1} in the voltage range of 2.0-4.8 V

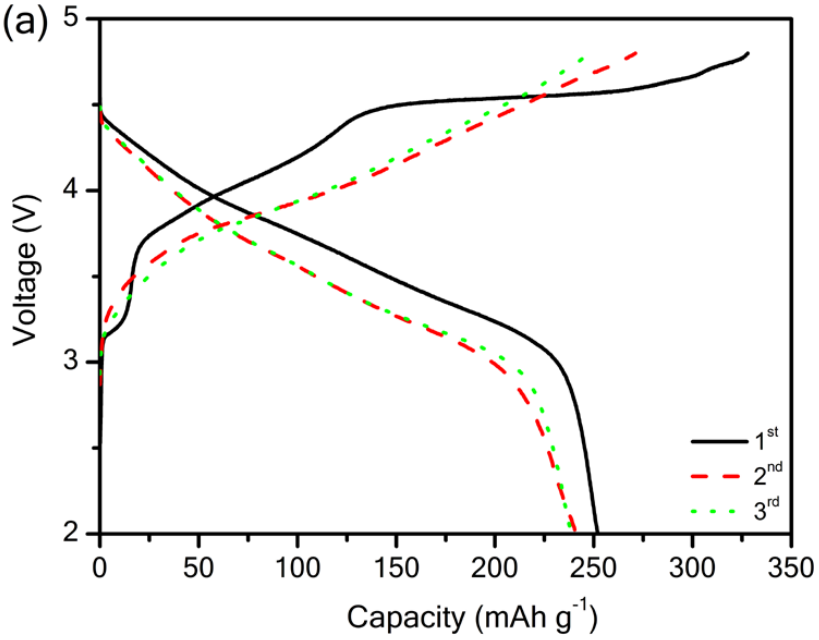

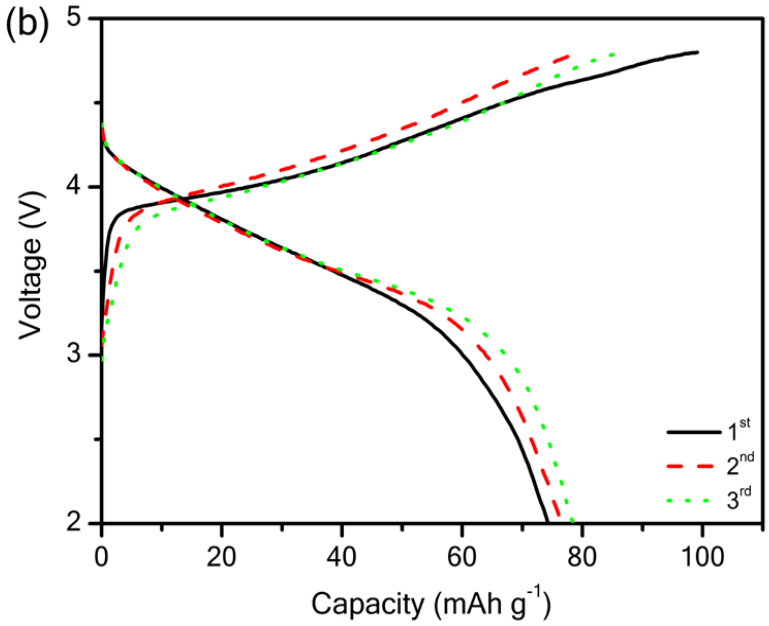

Figure 6. The first three charging/discharging plots of the (a) single- and (b) multiple-phases samples.

To illustrate the mechanism of the increasing capacity in the multiple-phases sample, the first three charging/discharging plots, and the XRD patterns of the samples after 1st and 6th cycles were given.

As shown in Fig. 6a, the single-phase sample shows two plateaus during initial charging process: one is caused by the oxidation of transition metal ions (< 4.45 V), and the other is due to the simultaneous release of lithium and oxygen as Li_2O when the charging voltage is up to 4.45 V. The later plateau can be responsible for the large IRC loss. Here, the IRC loss of the single-phase sample is about 80 mAh g^{-1}. In the subsequent cycles, the characteristic high-voltage charge plateau is associated with Li_2O disappears. Thackeray *et al.* [11] claimed that the chemical composite of Li-rich solid solution after initial cycle became $(0.4\text{-}\delta)Li_2MnO_3\cdot\delta MnO_2\cdot 0.4LiMO_2$.

Differing from the single-phase sample, the multiple-phases sample (see Fig. 6b) doesn't exhibit the high-voltage plateau (> 4.45 V) during the first charging process, and its IRC loss is around 25 mAh g^{-1}. In Belharouak *et al.*'s report [10], however, the sample with multiple phases showed two plateaus, and delivered a higher initial discharge capacity. The difference lies in the higher calcination temperature (1000 °C) in our experiments. At such high temperature, Li_2O could release from Li_2MnO_3 component (It is worthy to mention that if further increasing the calcination temperature to 1100 °C, we can clearly observe the white Li_2O impurity in the sample), yielding a multiple-phases sample of Li_2O-deficient layered Li-rich nickel manganese oxides, the chemical composition of which is analogous with $(0.4\text{-}\delta)Li_2MnO_3\cdot\delta MnO_2\cdot 0.4LiNi_{0.5}Mn_{0.5}O_2$ proposed by Thackeray *et al.* [11], and spinel $LiNi_{0.5}Mn_{1.5}O_4$. The high-temperature (55 °C) electrochemical test was also conducted, as shown in Fig. S2. It can be seen that the multiple-phases sample shows an increasing capacity with cycles in the initial several cycles, and it delivers an initial discharge capacity of 132 mAh g^{-1}. On the

high-temperature test, Li_2MnO_3 has been activated completely, and so there must be some other reasons for the phenomenon of increasing capacity.

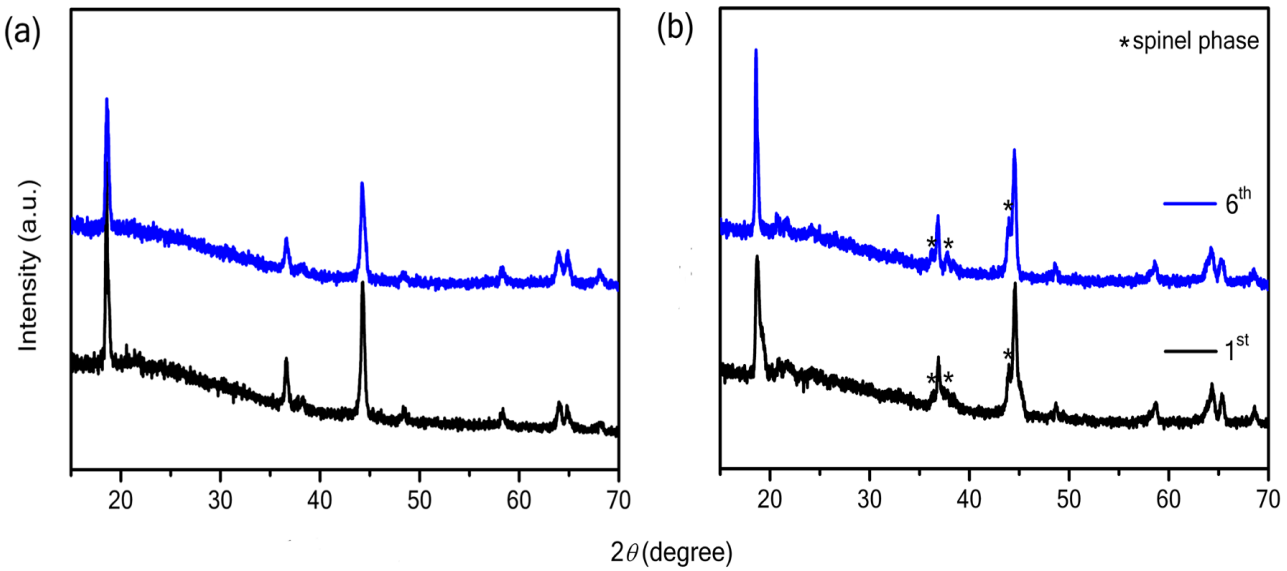

Figure 7. The XRD patterns of the (a) single- and (b) multiple-phases samples after 1st and 6th cycle

To reveal the electrochemical reactions occurred during the charge/discharge process, coin-type cells were disassembled in the glove box, and the cathode powders were scraped off from the Al foil and subsequently, washed with DMC and absolute ethanol for several times and then dried in vacuum. The cycled cathode material samples were characterized by XRD. The XRD patterns of the samples cycled for 1 and 6 times are shown in Fig. 7.

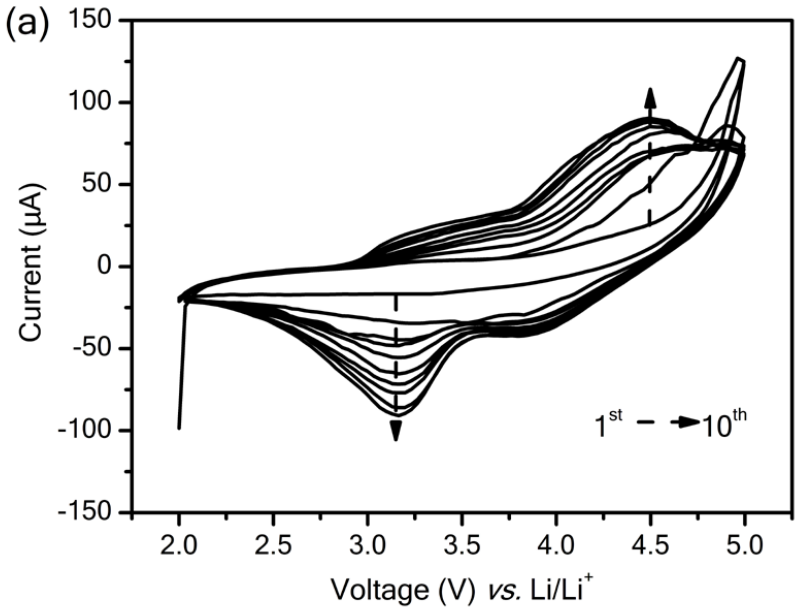

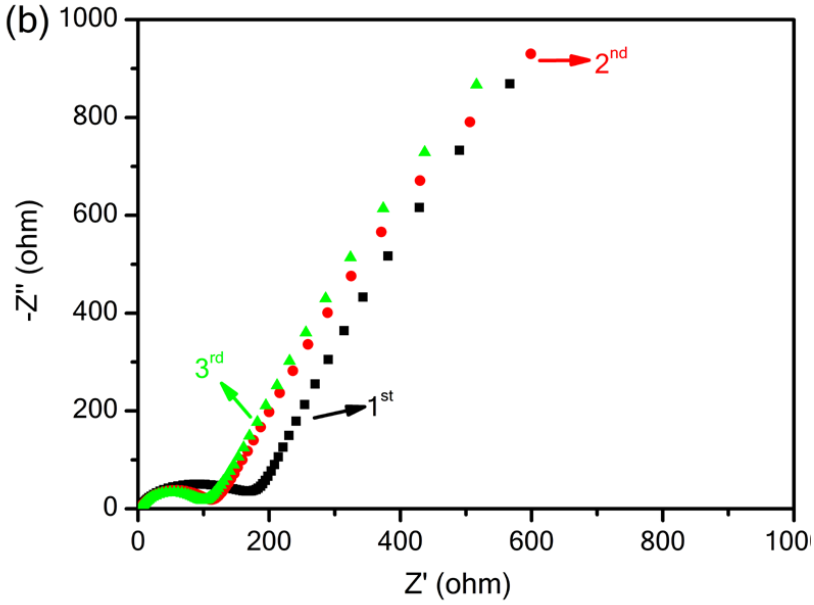

Figure 8. (a) Cyclic voltammograms from the first cycle to the tenth cycle, (b) electrochemical impedance spectroscopy after 1st, 2nd, 3rd charging/discharging process, of the multiple-phases sample

It can be found that the main phase of the single-/multiple- phases samples kept unchanged. Originally, we considered the rearrangement of the atomic sites during cycling resulted in the increasing capacity. Actually, from XRD results, there was no obvious evidence for the rearrangement of the atomic sites after cycling.

In order to further understand the mechanism of the phenomenon of increasing capacity, CV and EIS tests were carried out for the cells of the multiple-phases sample. It can be seen from Fig. 8a, the oxidation peaks below 3.5 V and above 3.8 V, which can be assigned to the redox reaction of Mn^{3+}/Mn^{4+} and Ni^{2+}/Ni^{4+} [20], grow and become more evident along with the increasing of cycle times. The high oxidation peak at around 5.0 V in the first cycle is due to the decomposition of the electrolyte. From the EIS results after initial 1st, 2nd, and 3rd cycles (Fig. 8b), we can see that the charge transfer resistance decreases with the cycles.

According to the above results, we have made an attempt to understand the lithium ion insertion behavior during the charge/discharge process of the multiple-phases sample in the cutoff voltage limits of 4.8 V to 2.0 V. For the fresh cathode, due to the lithium ion conduction pathways are different between outer spinel and inner layered structure, it is difficult for transporting lithium ion simultaneously. During the charge/discharge process, the lithium-ion located in the shell of spinel $LiNi_{0.5}Mn_{1.5}O_4$ firstly intercalated into anode, leaving Li^+ vacancies, and then the core of Li_2O-deficient Li-rich nickel manganese oxides. The conduction pathway was activated during cycling. The transition metal ions, such as Mn^{4+} and Ni^{2+} in the cathode material became more and more active as the number of intercalated/deintercalated lithium ion increased. As a result, the quantity of transition metal ions participating in the electrochemical reactions increased, and the charge resistance of the cell decreased. Consequently, the discharge capacity increased with the cycle. The more experimental evidences and theoretical calculations for our speculation on the phenomenon are ongoing.

4. CONCLUSIONS

A cathode material, with multiple phases of Li_2O-deficient layered Li-rich nickel manganese oxides and spinel $LiNi_{0.5}Mn_{1.5}O_4$, was prepared at 1000 °C. It was the evaporation and surface deficiency of lithium after high-temperature calcination that resulted in the phase separation of final product. For the multiple-phases sample, it had a relatively low IRC loss, due to the surface lixiviation of Li_2O from Li_2MnO_3 component; it exhibited a phenomenon of increasing capacity with cycle number in the initial several cycles both at 25 °C and 55 °C, which was proposed to be caused by the activation of lithium ion conduction pathway from inner layered structure to outer spinel structure; and also it delivered a high discharge capacity of 250 mAh g^{-1} after 50 cycles.

Electronic Supplementary Information:

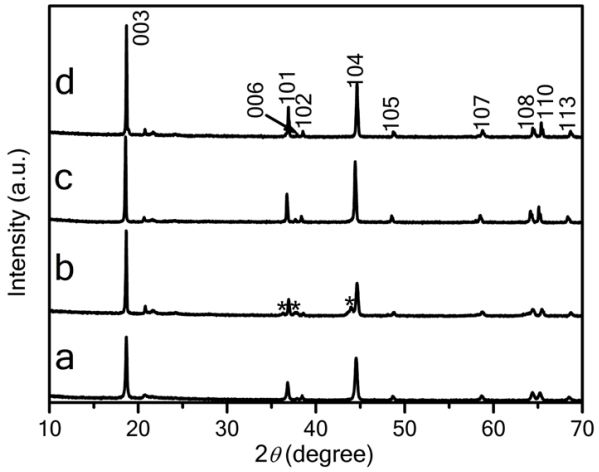

Figure S1. XRD patterns of $Li_{1.2}Ni_{0.2}Mn_{0.6}O_2$ samples prepared at (a) 900 °C, (b) 1000 °C, (c) 1000 °C with liquid nitrogen quenching, and (d) $Li_{1.2}Ni_{0.13}Co_{0.13}Mn_{0.54}O_2$ sample prepared at 1000 °C, based on a co-precipitation method

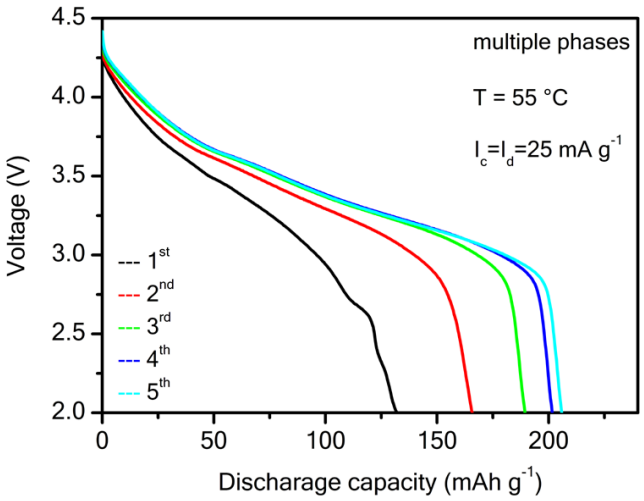

Figure S2. Initial five discharging plots of the multiple-phases sample at 55 °C

ACKNOWLEDGEMENTS
We are grateful for financial support from Zhejiang Provincial Natural Science Foundation of China (Grant No. R4100194 and Y4100499), and the Natural Science Foundation of Ningbo (Grant No. 2011A610201 and 2010A610150).

References

1. J. M. Tarascon and M. Armand, *Nature*, 414 (2001) 359
2. K. S. Kang, Y. S. Meng, J. Breger, C. P. Grey and G. Ceder, *Science*, 311 (2006) 977
3. P. Periasamy, N. Kalaiselvi and H. S. Kim, *Int. J. Electrochem. Sci.*, 2 (2007) 689
4. A.K. Padhi, K. S. Nanjundaswamy and J. B. Goodenough, *J. Electrochem. Soc.*, 144 (1997) 1188
5. Z. H. Lu, D. D. Macneil and J. R. Dahn, *Electrochem. Solid-State Lett.*, 4 (2001) A191
6. Z. H. Lu, L. Y. Beaulieu, R. A. Donaberger, C. L. Thomas and J. R. Danh, *J. Electronchem. Soc.*, 149 (2002) A778
7. J. Wang, X. Y. Yao, X. F. Zhou and Z. P. Liu, *J. Mater. Chem.*, 21 (2011) 2544
8. G. M. Koenig Jr., I. Belharouak, H. X. Deng, Y. K. Sun and K. Amine, *Chem. Mater.*, 23 (2011) 1954
9. Y. Wu and A. Manthiram, *Solid State Ionics*, 180 (2009) 50
10. I.Belharouak, G. M. Koenig Jr., J. W. Ma, D. P. Wang and K. Amine, *Electrochem. Commun.*, 13 (2011) 232
11. M. M. Thackeray, S. H. Kang, C. S. Johnson, J. T. Vaughey, R. Benedek and S. A. Hackney, *J. Mater. Chem.*, 17 (2007) 3112
12. S. H. Kang and K. Amine, *J. Power Sources*, 124 (2003) 533
13. L. Y. Yu, W. H. Qiu, F. Lian, J. Y. Huang and X. L. Kang, *J. Alloys. Compd.*, 471 (2009) 317
14. C. R. Fell, K. J. Carroll, M. F. Chi and Y. S. Meng, *J. Electrochem. Soc.*, 157 (2010) A1202
15. T. Ohzuku, M. Nagayama, K. Tsuji and K. Ariyoshi, *J. Mater. Chem.*, 21 (2011) 10179
16. T. Ohzuku, A. Ueda, M. Nagayama, Y. Iwakoshi and H. Komori, *Electrochim. Acta*, 38 (1993) 1159
17. M. Yoncheva, R. Stoyanova, E. Zhecheva, R. Alcantara, G. Ortiz and J. L. Tirado, *Electrochim. Acta*, 54 (2009) 1694
18. Y. C. Sun, Y. Shiosaki, Y. G. Xia and H. Noguchi, *J. Power Sources*, 159 (2006) 1353
19. S. Sivaprakash and S. B. Majumder, *Solid State Ionics*, 181 (2010) 730
20. S. Sivaprakash and S. B. Majumder, *J. Electrochem. Soc.*, 157 (2010) A418